First principles study of Nd energetics and diffusion in α U

Benjamin Beeler[a,*], Yongfeng Zhang[a]

[a]*Idaho National Laboratory, Idaho Falls, ID 83415*

Abstract

1. Introduction

Uranium-zirconium (U-Zr) and uranium-plutonium-zirconium (U-Pu-Zr) alloy fuels have a history of usage in sodium-cooled fast reactors. Not only does the U-Zr fuel (as well as U-Pu-Zr) generate a harder neutron spectrum as compared to traditional ceramic fuels, but it also offers excellent neutron economy and high burnup capability [1]. Recently, U-Zr fuels have regained interest due to the possibility of incorporating minor actinides into the fuel, and as such the metallic fuel alloys would serve to reduce the quantity of long-lived radioisotopes present in nuclear waste [2].

One issue with metallic fuels, including both UZr and UMo fuels, is the large amount of swelling that takes place [1]. Such swelling can be accounted for in the fuel design, however the swelling needs to be stable and predictable up to high fission densities. As shown in Fig. **??**, research reactor fuel types based on UMo are unique in that there cannot exist fission gas release from the fuel, and as such there is a relatively high content of fission gas and of fission gas bubbles within the fuel matrix. This importance of swelling in addition to the unique fuel environment has led to a variety of studies attempting to characterize the swelling behavior in U-Mo fuels [3, 4, 5, 6] which has led to the development of a swelling correlation from Argonne National Labortory (ANL correlation) [7] as a function of fission density. This swelling correlation was intended to be applicable for low temperature (less than 250°C) U-Mo alloys in the 7-10 wt.% composition range.

U-Zr alloys are typically employed as a series of fuel pellets within a given fuel rod, similar to UO_2 fuels. Unlike UO_2 fuels, dramatic swelling is inevitable, and is typically accounted for by manufacturing fuels with a smear density of approximately 75%. This allows for approximately 30% swelling, which is sufficient to allow fission gas release [8]. The nature of swelling is anisotropic in these fuels, largely due to the difference in swelling behavior between the hotter center of the fuel and the colder periphery [9]. The degree of anisotropicity increases with increasing Pu content. During operation, the phenomenon of constituent redistribution takes place. This results in three distinct radial regions within the fuel. The innermost region is Zr-rich, the intermediate region is Zr-poor and the outermost region has a nominal Zr

*Corresponding author
Email address: benjamin.beeler@inl.gov (Benjamin Beeler)

concentration. This phenomenon is due to both the effect of the temperature gradient on phase equilibria and the diffusion of species along the temperature gradient. This concentration variance as a function of radius in combination with the temperature gradient leads to the γ phase being present in the interior of the fuel pellet, while the α phase predominates the periphery [10, 11]. The radially anisotropic swelling within the fuel pellet is due to the variation in phases as a function of radius.

WIRTH TEXT *Metallicfuelsareidealforfast(breeder)reactorsbecausetheyproduceanextremelyhardneutronspectrum.*
ZrandU−Pu−Zralloysaretwoimportantpotentialmetallicfuelsforfastreactors.However,theswellingofmetallicfuelsism
oxidefuel,andisanimportantissueformetallicfuels.Fissionproductgas(Xe,Kr)bubblegrowthisbelievedtoberesponsiblefort
diffusioncanbeobtainedfromexperiments,theformationenergy,migrationbarrieranddiffusionmechanismsaredifficultt
principlesmethods[1?17],informationoninterstitialandvacancydiffusionisstilldeficient.Itisnecessarytopursuefurtherst
lamellae[18].Duetothelowertemperature,thebubblenucleationandgrowtharemoresevere.Inthispaper,wewillfocusonthe?ph
packedcorrugatedlayersofatoms,withlayersparalleltothe(010)planeandthecorrugationsparalleltothe[100]axis.Theself−
diffusionalongthe[010]directionisbelievedtobemuchmoredifficultthanintheothertwodirections[19].Theactivationenergyo
diffusioninpureuraniumalongallthreeprincipaldirectionshasbeenobtainedexperimentallyandisreportedas1.91eV[20]along
called?singlecrystalwithmosaicstructure?[20].Itshouldbesmallerthantheactualvalueduetothemosaicstructureofthesample
crystaluranium(1.91?2.91eV).Ontheotherhand,diffusionofinterstitialviaaninterstitialmechanismorinterstitialcymecha
outmechanism)isproposedtobenearlyisotropic,whichisseldominvestigatedintheliterature[29].Noexperimentalresultsofint
principlesmethods.However,bothofthemsufferfromunexpectedproblems,asdiscussedinsection2.Basedonourfirst−
principlescalculations,theformationenergyofthevacancyinpure?uraniumis1.69eV.Thediffusionofvacancyisalmostisotr
diffusionisthus2.03eValongthe[100]direction,2.05eValongthe[001]directionand2.93eValongthe[010]direction.Comparedw
principlescalculationresults.At612?C,theequilibriumconcentrationofZrin?Uisabout0.5%accordingtothephasediagram[31]
WIRTH TEXT

2. Computational Details

Systems are investigated using the Vienna *ab initio* Simulation Package (VASP) [12, 13, 14, 15]. The projector augmented wave (PAW) method [16, 17] is utilized within density functional theory [18, 19]. Calculations are performed using the Perdew-Burke-Ernzerhof (PBE) [20, 21] generalized gradient approximation (GGA) for the description of the exchange-correlation. Methfessel and Paxton's smearing method [22] of the first order is used with a width of 0.1 eV to determine partial occupancies for each wavefunction. Wavefunction optimization was truncated when the energy difference was less than 10^{-5} eV. The optimization procedure was truncated when the residual forces for the relaxed atoms were less than 0.01 eV/Å. Symmetry is switched off for all calculations. A support grid is utilized for the evaluation of augmentation charges. Non-spherical contributions from the gradient corrections inside the PAW spheres are included. Convergence testing was performed for this system in the model of Huang and Wirth [23] (utilized Perdew-Wang (PW91) [24, 25] GGA). The energy cutoff is increased, the supercell is increased in size, and the k-points mesh is refined until the energy of the pure system and the formation energy of a vacancy vary by less than 5 meV.

The convergence testing led to the choice of a 252 atom supercell (7x3x3 unit cells), a cutoff energy of 400 eV and a gamma-centered k-points mesh of 4x2x4, resulting in 20 k-points in the irreducible part of the Brillouin zone. The calculated lattice parameters are $a = 2.803$ Å, $b = 5.836$ Å, $c = 4.906$ Å and $y = 0.098$. These results compare very favorable to previous results [23, 26, 27] and experiments [28].

In order to obtain migration barriers for the various pathways investigated, we utilized the climbing-image nudged elastic band (CI-NEB) method [29]. Both single and multiple image implementations of the CI-NEB method were implemented to ensure that both the correct migration pathway and the correct migration barrier magnitude were obtained.

3. Results

3.1. Defect formation energies in αU

To verify the methodologies presented in this study, the formation energy of a single vacancy and a single interstitial in αU were calculated utilizing equation 1 and 2, respectively,

$$E_f^{vac} = E_{vac} - (n-1) * E_{pure} \tag{1}$$

$$E_f^{int} = E_{int} - (n+1) * E_{pure} \tag{2}$$

where E_{vac} is the total energy of the system with a vacancy, E_{int} is the total energy of the system with an interstitial, E_{pure} is the energy per atom of a defect-free system, and n is the number of atoms in the defect-free system. The vacancy formation energy is calculated to be 1.70 eV, which compares very favorably with the calculations of Huang and Wirth [23] (1.69 eV).

Nd interstitial 7.8 eV. A Nd substitutional of 2.106 eV and U interstitial of 4.31 eV [30] have a lower combined energy than the Nd interstitial. Thus it would be expected that if a Nd interstitial is created, it would transform into a substitutional Nd atom and create a U SIA. Therefore, only vacancy-mediated diffusion of Nd atoms is investigated. Also, vacancy migration in the corrugated plane in four time as likely (migration barriers of 1.24 eV out of corrugated plane, 0.36 eV and 0.34 eV in corrugated plane [23], thus only vacancy migration in the corrugated plane is investigated.

Table 1: Formation energies for vacancy-Nd defects in alpha U.

Defect	E_{form}
vacancy	1.701
Nd sub	2.106
Nd Vac X	2.886
Nd Vac Z	2.627

Needs Nd-vac binding energies??

Table 2: Formation energies of multi-vacancy defect complexes in alpha U

Defect	E_{form}
Divac X	3.835
Divac Z	3.638
Divac 2nn X	3.377
Divac 2nn Z	3.616
Nd Divac X	4.845
Nd Divac Z	4.161
Nd Divac XZ	4.081
Trivac X	5.858
Trivac Z	5.553
Trivac XZ	5.549

Table 3: Formation energies of Nd and Pd point defects in alpha U.

Defect	E_{form}
Pd sub	0.218
NdPd X	-1.709
NdPd Z	-1.705
Pd Vac X	1.693
Pd Vac Z	1.627

Nd with vac Z - sits slightly off of lattice site, as shown in Figure 1.

Nd with vac X - sits in middle of two lattice sites, as shown in Figure 2.

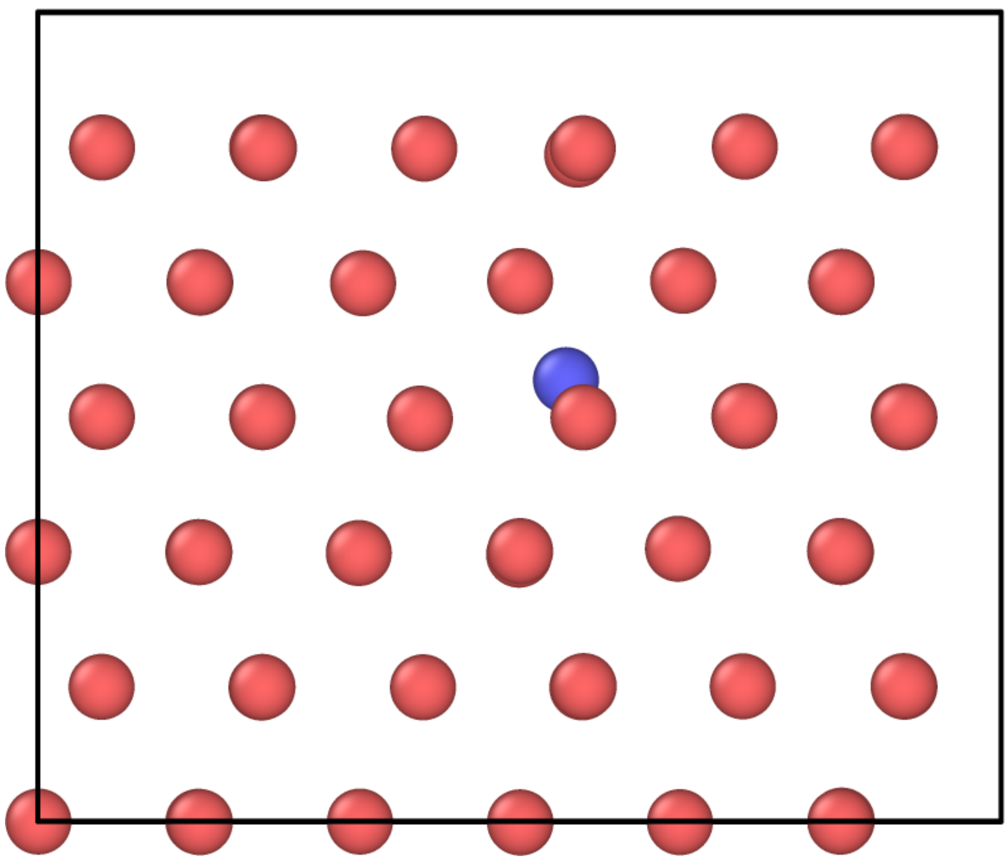

Figure 1: 2D projection of a slice of the relaxed structure of Nd atom inserted into α U as a substitutional with a nearest-neighbor vacancy (positive z axis) in the corrugated plane. View is (100) plane.

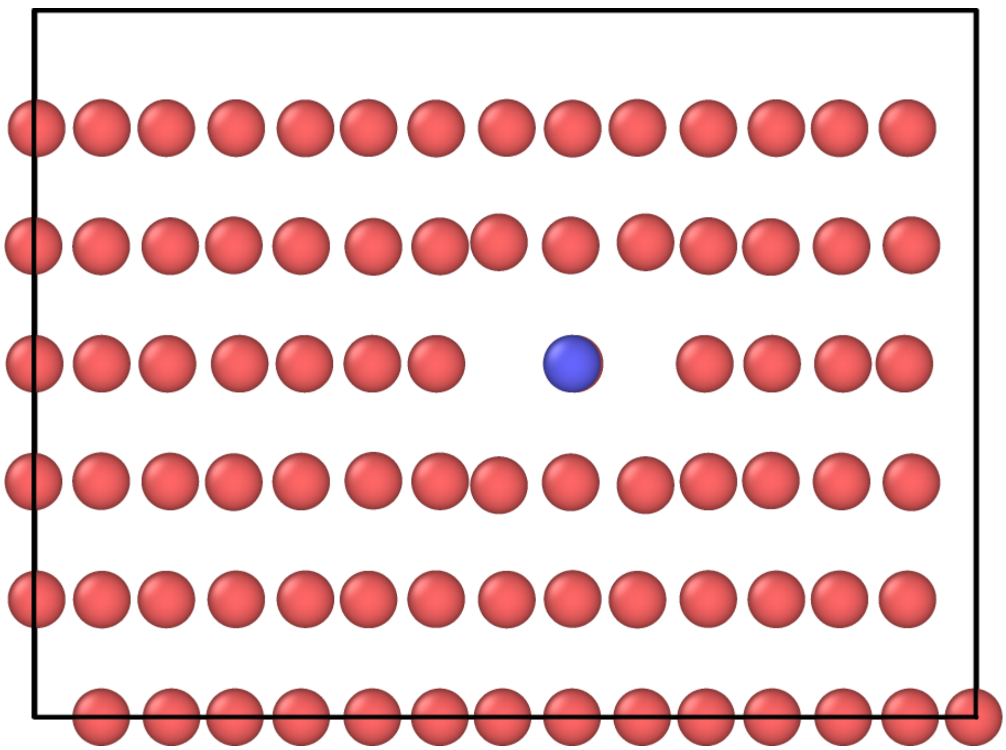

Figure 2: 2D projection of a slice of the relaxed structure of Nd atom inserted into α U as a substitutional with a nearest-neighbor vacancy (positive x axis) in the corrugated plane. View is (010) plane.

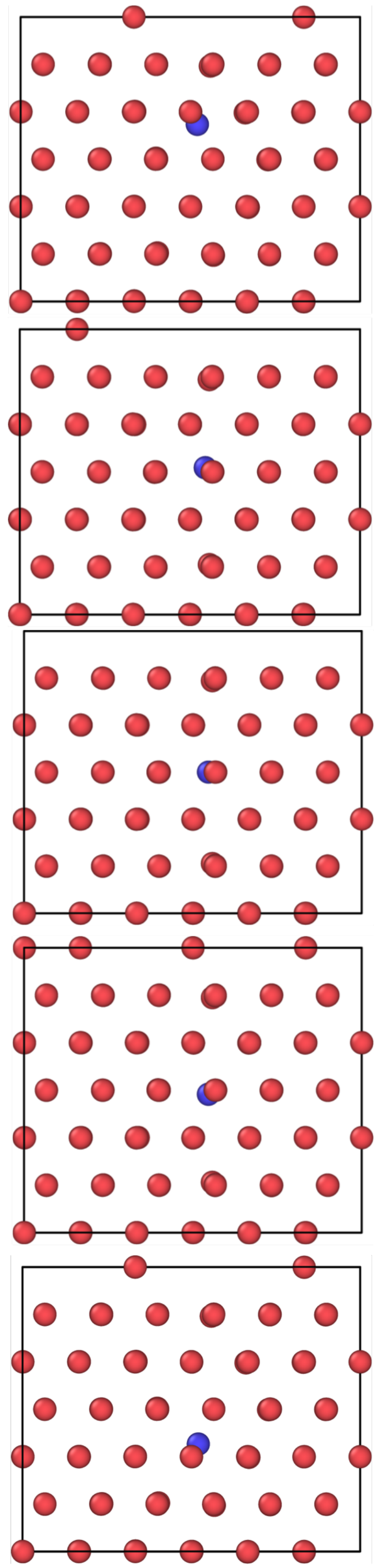

Figure 3: Schematic of Nd atom diffusion within a Nd-divacancy complex.

4. Conclusions

5. Acknowledgement

[1] G. Hofman, L. Walters, T. Bauer, Metallic fast reactor fuels, Progress in Nuclear Energy 31 (1997) 83.

[2] L. Capriotti, S. Bremier, K. Inagaki, P. Poml, D. papaioannou, H. Ohta, T. Ogata, V. Rondinella, Characterization of metallic fuel for minor actinides transmutation in fast reactor, Progress in Nuclear Energy 94 (2017) 194.

[3] J. Rest, G. Hofman, Y. Kim, Analysis of intergranular fission-gas bubble-size distributions in irradiated uranium-molybdenum alloy fuel, J. Nucl. Mater. 385 (2009) 563.

[4] Y. Kim, G. Hofman, J. Rest, G. Shevlyakov, Characterization of intergranular fission gas bubbles in u-mo fuel, Tech. Rep. ANL-08/11, Argonne National Laboratory (2008).

[5] M. Meyer, G. Hofman, S. Hayes, C. Clark, T. Wiencek, J. Snelgrove, R. Strain, K. Kim, Low-temperature irradiation behavior of uranium-molybdenum alloy dispersion fuel, J. Nucl. Mater. 304 (2002) 221.

[6] Y. Kim, G. Hofman, J. Cheon, A. Robinson, D. Wachs, Fission induced swelling and creep of u-mo alloy fuel, J. Nucl. Mater. 437 (2013) 37.

[7] Y. Kim, G. Hofman, Fission product induced swelling of u-mo alloy fuel, J. Nucl. Mater. 419 (2011) 291.

[8] W. Beck, R. Fousek, J. Kittel, The irradiation behavior of high-burnup uranium-plutonium alloy prototype fuel elements, Tech. Rep. ANL-7388, Argonne National Laboratory (1968).

[9] G. Hofman, R. Paul, C. Lahm, D. Porter, Swelling behavior of u-pu-zr fuel, Metall. Trans. A 21A (1990) 517.

[10] T. Kobayashi, M. Kinoshita, S. Hattori, Development of the sesami metallic fuel performance code, Nucl. Tech. 89 (1990) 183.

[11] Y. Kim, G. Hofman, S. Hayes, Y. Sohn, Constituent redistribution in u–pu–zr fuel during irradiation, J. Nucl. Mater. 327 (2004) 27.

[12] G. Kresse, J. Hafner, Ab initio molecular dynamics for liquid metals, Phys. Rev. B 47 (1993) 558.

[13] G. Kresse, J. Hafner, Ab initio molecular-dynamics simulation of the liquid-metal-amorphous-semiconductor transition in germanium, Phys. Rev. B 49 (1994) 14251.

[14] G. Kresse, J. Furthmuller, Efficiency of ab-initio total energy calculations for metals and semiconductors using a plane-wave basis set, Comput. Mat. Sci. 6 (1996) 15.

[15] G. Kresse, J. Furthmuller, Efficient iterative schemes for ab initio total-energy calculations using a plane-wave basis set, Phys. Rev. B 54 (1996) 11169.

[16] P. Blochl, Projector augmented-wave method, Phys. Rev. B 50 (1994) 17953.

[17] G. Kresse, D. Joubert, From ultrasoft pseudopotentials to the projector augmented-wave method, Phys. Rev. B 59 (1999) 1758.

[18] P. Hohenberg, W. Kohn, Inhomogeneous electron gas, Phys. Rev. 136 (1964) B864.

[19] W. Kohn, L. Sham, Self-consistent equations including exchange and correlation effects, Phys. Rev. 140 (1965) A1133.

[20] J. Perdew, K. Burke, M. Ernzerhof, Generalized gradient approximation made simple, Phys. Rev. Lett. 77 (1996) 3865.

[21] J. Perdew, K. Burke, M. Ernzerhof, Erratum: Generalized gradient approximation made simple, Phys. Rev. Lett. 78 (1997) 1396.

[22] M. Methfessel, A. Paxton, High-precision sampling for brillouin-zone integration in metals, Phys. Rev. B 40 (1989) 3616.

[23] G.-Y. Huang, B. Wirth, First-principles study of diffusion of interstitial and vacancy in alpha u-zr, J. Phys.: Cond. Mat. 23 (2011) 205402.

[24] J. Perdew, J. Chevary, S. Vosko, K. Jackson, M. Pederson, D. Singh, C. Fiolhais, Atoms, molecules, solid and surfaces: Applications of the generalized gradient approximation for exchange and correlation, Phys. Rev. B 46 (1992) 6671.

[25] J. Perdew, J. Chevary, S. Vosko, K. Jackson, M. Pederson, D. Singh, C. Fiolhais, Erratum: Atoms, molecules, solid and surfaces: Applications of the generalized gradient approximation for exchange and correlation, Phys. Rev. B 48 (1993) 4978.

[26] P. Soderlind, First-principles elastic and structural properties of uranium metal, Phys. Rev. B 66 (2002) 085113.

[27] C. Taylor, Evaluation of first-principles techniques for obtaining materials parameters of alpha uranium and the (001) alpha uranium surface, Phys. Rev. B 77 (2008) 094119.

[28] C. Barrett, H. Mueller, R. Hitterman, Crystal structure variations in alpha uranium at low temperatures, Phys. Rev. 129 (1963) 625.

[29] G. Henkleman, G. Johannesson, H. Jonsson, A climbing image nudged elastic band method for finding saddle points and minimum energy paths, J. Chem. Phys. 113 (2000) 9901.

[30] G.-Y. Huang, B. Wirth, First-principles study of bubble nucleation and growth behaviors in alpha u-zr, J. Phys.: Cond. Mat. 24 (2012) 415404.